Published in final edited form as:
J Magn Reson Imaging. 2013 May ; 37(5): 1100–1108. doi:10.1002/jmri.23906.

In vivo Validation of 4D Flow MRI for Assessing the Hemodynamics of Portal Hypertension

A Roldán-Alzate, PhD[1,2], **A Frydrychowicz, MD**[1], **E Niespodzany, MS**[1,2], **BR Landgraf, BS**[1,2], **KM Johnson, PhD**[2], **O Wieben, PhD**[1,2], and **SB Reeder, MD, PhD**[1,2,3,4]

[1]Department of Radiology, University of Wisconsin – Madison

[2]Department of Medical Physics, University of Wisconsin – Madison

[3]Department of Medicine, University of Wisconsin – Madison

[4]Department of Biomedical Engineering, University of Wisconsin – Madison

Abstract

Purpose—to implement and validate in vivo radial 4D flow MRI for quantification of blood flow in the hepatic arterial, portal venous and splanchnic vasculature of healthy volunteers and patients with portal hypertension.

Methods & Materials—17 patients with portal hypertension and 7 subjects with no liver disease were included in this HIPAA-compliant and IRB-approved study. Exams were conducted at 3T using a 32-channel body coil with large volumetric coverage and 1.4mm isotropic true spatial resolution. Using post-processing software, cut-planes orthogonal to vessels were used to quantify flow (L/min) in the hepatic and splanchnic vasculature.

Results—Flow quantification was successful in all cases. Portal vein and supra-celiac aorta flow demonstrated high variability among patients. Measurements were validated indirectly using internal consistency at three different locations within the portal vein (error=4.2±3.9%) and conservation of mass at the portal confluence (error=5.9±2.5%) and portal bifurcation (error=5.8±3.1%).

Discussion—This work demonstrates the feasibility of radial 4D flow MRI to quantify flow in the hepatic and splanchnic vasculature. Flow results agreed well with data reported in the literature, and conservation of mass provided indirect validation of flow quantification. Flow in patients with portal hypertensions demonstrated high variability with patterns and magnitude consistent with the hyperdynamic state that commonly occurs in portal hypertension.

Keywords

4D Flow MRI; Hepatic Hemodynamics; Portal Hypertension

Please address correspondence to: Alejandro Roldán-Alzate, Ph.D, Department of Radiology, University of Wisconsin - Madison, B1141 WIMR, Madison, Wisconsin 53705, roldan@wisc.edu.

Financial disclosures: The Departments of Radiology and Medical Physics receive support by GE Healthcare.

Introduction

Cirrhosis is the common, end-stage pathway of chronic liver disease leading to the mortality of more than 30,000 people in the United States each year (1). Portal hypertension is the most common and most lethal complication in patients with cirrhosis (1). Dramatic alterations in blood flow occur in patients with cirrhosis during the development of portal hypertension. Initially, there is a progressive increase in vascular resistance at the sinusoidal level due to passive resistance caused by architectural changes related to fibrosis, and active resistance related to vasoconstriction of vascular smooth muscle cells in the liver (2). As the disease progresses, endogenous release of vasodilators attempts to maintain flow in the liver, leading to systemic hypotension. This can lead to compensatory hyperdynamic circulation and paradoxically, increased portal flow that leads to further increases in the porto-systemic pressure gradient (3-5).

The best-validated biomarker of portal hypertension is the hepatic venous pressure gradient (HVPG), which is the pressure difference between the portal vein and the inferior vena cava (IVC) (6,7). HVPG plays a central role not only in diagnosis, but also for treatment monitoring of portal hypertension(8-12). Unfortunately, measurement of HVPG is invasive, typically performed by placement of a balloon catheter in the right hepatic vein, via the internal jugular vein, where the difference between the wedged venous pressure and systemic venous pressure is used to estimate HVPG (13-16).

HVPG [mmHg] is the product of blood flow and resistance of the portal circulation, ie. $HVPG = Q \times R$. Thus, non-invasive measurement of portal flow (Q), may serve as an important surrogate biomarker for portal hypertension. Indeed, in patients with advanced cirrhosis, flow is the primary determinant of portal pressure. This is largely due to the high levels of circulating endogenous vasodilators that lead to an elevated cardiac output that increases portal blood flow (Q), paradoxically exacerbating portal hypertension (17). It is for this reason that most pharmacological and interventional therapies, such as transjugular intrahepatic portosystemic shunt (TIPS), aim to reduce portal pressure by reducing or redirecting flow to the systemic venous circulation (10,18-23). For this reason, measurement of portal flow holds tremendous potential as a central parameter to characterize response to treatment.

Unfortunately, non-invasive assessment of the hepatic and splanchnic vasculature is challenging. Doppler ultrasound (US) is the most commonly used diagnostic tool for noninvasive assessment of the portal circulation (24). US can measure flow velocity within the main portal circulation, but can only be performed in large vessels (eg. main portal vein). In addition, flow quantification is estimated from the average velocity and vessel cross-sectional area. Furthermore, collateral pathways associated with portal hypertension are highly variable and extend throughout the abdomen. Because of overlying intestinal gas, US is often limited for visualization of variceal flow (25,26). Finally, flow measurements within the portal vein using ultrasound have been shown to be highly variable demonstrating 69% variability in repeatability experiments (27).

Conventional flow sensitive MRI using 2D slice selection, cardiac gating, and phase contrast (PC) velocity encoding is an excellent alternative to measure blood flow within the abdomen (5,28,29). However, 2D PC MR requires the use of double-oblique imaging planes that are challenging and time consuming to position and coordinate with patient breath-holding. Indeed, the acquisition of numerous 2D planes for comprehensive flow evaluation of the hepatic vasculature is not feasible in a clinical scenario.

4D magnetic resonance velocity mapping using temporally resolved 3D spatial encoding ("4D"), offers the unique combination of co-registered anatomic and hemodynamic visualization in a single exam. Initial hemodynamic analysis of the portal vein by Stankovic et al. using a Cartesian 4D velocity mapping approaching are highly promising(30). Unfortunately, the spatial resolution and coverage in this approach is limited to assessment of flow to large vessels and precluded to assessment of anomalous or collateral flow pathways. Further, a single velocity encoding (venc) setting limited evaluation of flow to the portal and splanchnic venous vasculature. Recent work by Frydrychowicz et al. demonstrated feasibility of qualitative flow visualization with high spatial resolution and large volumetric coverage using 3D radial undersampling strategies (31). However, as with other accelerated imaging strategies, there is potential for inaccuracies in flow measurements, which have not been assessed for hepatic flow. Therefore, the purpose of this study is to implement and validate in vivo radial 4D flow MRI for quantification of blood flow quantification in the hepatic arterial, portal venous and splanchnic vasculature of healthy volunteers and patients with portal hypertension.

Methods & Materials

Human subjects

7 controls with no history of liver disease (32.2±10.1 years, 85.7±8.7 kg; 4 male, 3 female) were recruited for this (Health Insurance Portability and Accountability Act) HIPAA-compliant and (Institutional Review Board) IRB-approved study. Further, 17 subjects with a clinical history of cirrhosis and portal hypertension were recruited (58.6±6.73 years; 88.4± 6.7 kg; 13 male, 4 female). Diagnosis of cirrhosis was based on past medical history, and diagnosis of portal hypertension was determined either by clinical history or from imaging features of portal hypertension (eg. varices, splenomegaly) from clinical MRI studies. Written informed consent was obtained from all participants prior to inclusion. All subjects were asked to fast for at least 3 hours prior to the MRI examination.

MR Imaging

MR images were acquired on a 3T scanner (Discovery MR 750, GE Healthcare, Waukesha, WI) with a 32-channel phased array body coil (NeoCoil, Pewaukee, WI). A balanced 5-point velocity encoded PC-VIPR sequence was used to provide time-efficient, large volume coverage with high spatial and temporal resolution and increased velocity encoding sensitivity (32,33). Imaging parameters used for the patients included: dual echo acquisition, excitation volume=32cm A/P × 32cm R/L × 22cm S/I, achieving true acquired spatial resolution of 1.4mm isotropic, TR/TE=6.1-6.7/2.1-2.5ms (first echo), flip angle=8-10°, and venc=60cm/s. One of the healthy subjects was scanned using the same parameters used for

the patients. The remaining six healthy subjects used flip angle=15°, and venc=100cm/s. An adaptive respiratory gating scheme using respiratory bellows and a 50% acceptance window resulted in scan times of approximately 10-12min depending on the respiratory rate of the subject(34). Retrospective ECG gating with temporal filtering (35) similar to view sharing in Cartesian acquisitions was used.

Data were reconstructed to 14 time frames per RR cycle. Phase offsets for Maxwell terms and eddy currents were corrected automatically during reconstruction (36,37). The eddy current correction was performed with 2nd order polynomial fitting of background tissue segmented based on thresholding of an angiogram (37). In all patients, studies were performed concluding a conventional clinical liver MRI exam. Per clinical standard, 0.1mmol/kg gadobenate dimeglumine (Bracco Diagnostics, Princeton, NJ) was injected at a flow rate of 2 mL/s by means of a 20G antecubital i.v. line, and imaging with radial 4D flow MRI was performed approximately 10 minutes after the injection of contrast. The same contrast agent injection scheme was used in the normal subjects.

Velocity-weighted angiograms were calculated from the final velocity and magnitude data for all 14 time frames (38). Subsequent vessel segmentation was performed using commercial segmentation software (MIMICS, Materialise, Leuven, Belgium). Segmented images were imported into a commercially available velocity field visualization software (EnSight, CEI Inc., Apex, NC). Utilizing the angiogram as a guide for locations, cut-planes perpendicular to the axis of flow were created in the following vessels: main portal vein (PV), both main portal vein branches (ltPV, rtPV), splenic vein (SV), superior mesenteric vein (SMV), abdominal aorta (Ao) and proper hepatic artery (HA) (flow in accessory hepatic arteries was also quantified when anomalous hepatic arteries or anatomical variations on it were present). Flow quantification was performed by exporting cut-plane information to a previously described program written in Matlab (Mathworks, Natick, MA) (39). Figure 1 diagrams the post-processing workflow.

In addition, the accuracy and internal consistency of the flow measurements were indirectly validated based on the concept of continuity (conservation of mass) in all cases. This was performed by measuring blood flow through the PV at three adjacent locations spaced approximately 1cm apart. In addition, conservation of mass was tested at the portal confluence and bifurcation by measuring blood flow in the splenic vein (Q_{SV}), superior mesenteric vein (Q_{SMV}), and right and left portal veins (Q_{RPV}) and (Q_{LPV}) respectively, such that

$$Q_{SV}+Q_{SMV}=Q_{PV}=Q_{RPV}+Q_{LPV} \quad (1)$$

as shown schematically in Figure 2. Finally, quantification in all vessels was performed by two independent observers for 6 of the volunteers to determine inter-observer variability using Bland-Altman-analysis. Further, one of the observers repeated the measurements on a second day to test for intra-observer variability, also using Bland-Altman-analysis.

Results

The underlying diseases in the 17 patients were as follows: six (6) patients had cirrhosis related to hepatitis C, one (1) had cirrhosis related to both hepatitis B and C, four (4) had alcoholic cirrhosis, two (2) had cirrhosis from non-alcoholic fatty liver disease (NAFLD), one (1) had cirrhosis related to primary sclerosis cholangitis, one (1) with cirrhosis as a complication of chronic bile stasis from a remote hepatojejunostomy, and finally one (1) severe steatosis.

Radial 4D flow MRI was successfully performed in all subjects (~ 10-12 minutes of free breathing depending on the respiratory pattern). Figure 3 shows volume rendered angiographic 4D flow MR images demonstrating the complex vascular anatomy of the liver in a normal subject. Large anatomical coverage and the wide range of velocities provided by the 5-point velocity encoding method make this technique sufficiently robust to identify all vessels in all vascular territories, including both arterial, portal venous and venous blood flow. Anatomical variations resulting from the collateral circulation in three (3) of the patients with portal hypertension are shown in Figure 4. Two patients and two healthy subjects had anomalous or accessory hepatic arteries, which were also quantified for the analysis.

Figure 5 shows the quantification of blood flow in the portal vein (Q_{PV}), hepatic artery (Q_{HA}) and abdominal aorta (Q_{Ao}). On average, blood flow through the portal vein was lower in patients with portal hypertension (1.09 ± 0.8 L/min; range = -0.4 – 3.2 L/min) compared to healthy volunteers (1.1 ± 0.4 L/min; range = 0.9 – 2.1 L/min), although this difference was not statistically significant (p=0.6) (Fig. 5). In addition, high variability in portal venous flow was observed in the subjects with portal hypertension, suggesting that some of these patients were in a hyperdynamic state. Two of the PH patients showed abnormal flow regimes in portal circulation (* and ** in Fig. 5). Flow profiles in these two cases are shown in Figure 6. Vectors indicate the direction of the flow and streamline colors represent the magnitude of the velocity.

Blood flow through the hepatic artery was lower in patients (0.19 ± 0.13 L/min; range = 0.06 – 0.48 L/min) than that in healthy volunteers (0.2 ± 0.09 L/min; range = 0.08 – 0.33 L/min), although the difference in Q_{HA} was small and not statistically significant (p=0.9). Total blood flow to the liver ($Q_{PV} + Q_{HA}$) was lower in patients with portal hypertension (1.28 ± 0.85 L/min; range = -0.11 – 3.61 L/min) than in healthy volunteers (1.47 ± 0.39 L/min; range = 1.01 – 2.26 L/min) (p=0.56), however the difference was not statistically significant as expected based on what was seen in the individual flows (Q_{PV} and Q_{HA}).

Blood flow through the abdominal aorta in the supra-celiac anatomical location was measured to evaluate for hyperdynamic state and the influence of cardiac output on hepatic and splanchnic flow. Q_{Ao} was not significantly different between PH patients (3.8 ± 1.6 L/min; range = 2.0 – 7.2 L/min) and healthy volunteers (3.5 ± 0.6 L/min; range = 2.7 – 4.5L/min) (p=0.9) however, similar to what was observed in the portal vein flow, high variability was observed in the patients with portal hypertension (Fig 5).

The effects of cardiac output were accounted for by normalizing the portal venous and hepatic arterial blood flows by the flow through the abdominal aorta, which quantifies the cardiac output delivered to the lower body. Results are plotted in Figure 6, demonstrate remarkably reduced variability in both the hepatic and portal venous flow, indicating that differences in flow in patients with portal hypertension are largely due to difference in cardiac output related to a variable presentation of patients with a hyperdynamic state.

The portal vein and hepatic artery fractions of the blood flow to the liver were calculated by dividing each specific contribution by the total blood flow to the liver and are shown in Figure 6. The portal fraction ($PV_{Fraction} = Q_{PV} /(Q_{PV} + Q_{HA})$) in patients (83.6 ± 15.8 %; range = 31.8 – 96 %) was lower than that in the healthy volunteers (86.3 ± 6 %; range = 78.2 – 93.7 %), however no significant difference was found between the two groups (p =0.6). Since the hepatic artery fraction ($HA_{Fraction}$) is equal to 1 – PV%, the contribution of the hepatic artery was not significantly different between the two groups either.

The accuracy of the measurements was validated indirectly using internal consistency and conservation of mass principles. First, measurement of Q_{PV} at three different locations in the portal vein revealed an average absolute error of 4.2 ± 3.9 %. Second, comparison of flow into the portal confluence ($Q_{SV} + Q_{SMV}$) with the flow in the portal vein (Q_{PV}) demonstrated an error of 5.9 ± 2.5% and the comparison of flow in the portal bifurcation ($Q_{RPV} + Q_{LPV}$) showed an error of 5.8 ± 3.1. Comparison of blood flow at the portal confluence and at the portal vein demonstrated excellent correlation (r^2 of 0.99) with slope (m = 0.94 ± 0.01, p=0.0005) and intercept (b = 0.27± 0.2 ml/cylce, p=0.23) very close to 1 and 0, respectively, indicating good agreement between the two measurements (Fig. 8.a). Additionally, the comparison between blood flow measurements at the portal vein and at the bifurcation also demonstrated excellent correlation ($r^2 = 0.99$) with slope (m = 0.96 ± 0.01, p=0.04) and intercept (b = -0.05 ± 0.27 ml/cycle, p=0.85) very close to 1 and 0, respectively, indicating good agreement of the two measurements of flow (Fig. 8.b). Bland-Altman analysis for these two comparisons showed very low bias. For the portal confluence, bias was 0.58 ml/cycle, with 95% limits of agreement spanning -1.14 to 2.30 ml/cycle. For the portal bifurcation, the corresponding bias was 0.66 ml/cycle, with -1.18 to 2.50 ml/cycle 95% limits of agreement.

Inter-observer variability calculated using Bland-Altman analysis showed a very low bias between readers. For hepatic arterial flow, bias (mean difference) was 0.018 L/min, with 95% limits of agreement spanning -0.150 to 0.186 L/min; for portal venous flow the corresponding bias was 0.032 L/min, with -0.022 to 0.086 L/min 95% limits of agreement. Overall, the inter-observer bias was 3% of the average portal venous flow and 10% of the average hepatic arterial flow.

Intra-observer variability calculated using Bland-Altman analysis, showed very low bias. For the hepatic arterial flow, bias was –0.007 L/min, with 95% limits of agreement spanning -0.020 to 0.006 L/min; for portal venous flow the corresponding bias was 0.011 L/min, with -0.018 to 0.004 L/min 95% limits of agreement. Overall, the intra-observer bias was 1% of the average portal venous flow and 4% of the average hepatic arterial flow.

Discussion

This study demonstrates the feasibility of using radial 4D flow MRI to quantify blood flow in the hepatic and splanchnic vasculature of healthy volunteers and patients with portal hypertension. Volumetric 4D flow MRI velocity acquisition of the whole abdomen was performed with very high spatial resolution in a single free-breathing 10-12 minutes scan. Good internal consistency tested through conservation of mass, as well as good inter- and intra-observer variability demonstrates the potential of this approach to quantify blood flow to the liver in the setting of portal hypertension.

This approach not only allows the detection and characterization of blood flow patterns and quantification of blood flow but also has large volumetric coverage. Volumetric coverage with high spatial resolution partially addresses known limitations of Doppler ultrasound, such as operator dependence, limited acoustic windows, visualization of complex anatomy, and the limited inter- and intra- observer reproducibility of ultrasound (24). Even though Doppler ultrasound can provide velocity measurements in the vessels of interest, it is often limited in its ability to accurately measure cross-sectional area and hence true flow through the vessel (40). By measuring a volumetric velocity map, the 4D flow method can provide true flow measurements in any vessel included in the volume. This approach also avoids the need to acquire numerous double oblique planes needed for 2D phase contrast MRI methods. Volumetric velocity mapping has shown to be well suited for the liver and abdomen vasculature where one comprehensive acquisition is followed by post-processing and flow measurements in specific vessels (31).

Comprehensive quantitative analysis of hepatic hemodynamics in patients with liver disease offers several unique and important diagnostic opportunities. For example, after a meal challenge, the increased blood flow that occurs in the postprandial state affects the entire hepatic vasculature. Changes in portal venous blood flow in response to meal ingestion, has been reported as an indicator of the severity of cirrhosis and portal hypertension (41). In the presence of portosystemic collaterals, this response may vary significantly (42) and such additional pathways should be assessed as well, preferably in the same examination. The large volumetric coverage facilitated by radial 4D flow MRI offers new opportunities for comprehensive and quantitative evaluation of portosystemic collaterals in addition to the portal venous and arterial circulation of the abdomen.

In this study, the main differences observed between portal hypertension patients and healthy volunteers was the high variability of blood flow through the portal vein observed patients. The best explanation for this variability is variability in cardiac output with a variable presentation of patients in a hyperdynamic state(17). Indeed, after flow measurements were normalized by the flow measured in the abdominal aorta (as a surrogate for cardiac output), the variability was greatly reduced. This observation also demonstrates that comprehensive characterization of blood flow to the liver may also require measurement of flow in the aorta. The ability to measure flow in the aorta as part the same exam is a unique advantage of the 4D flow MRI compared to the liver.

In addition, the relative contribution of portal venous flow and hepatic artery flow to the total liver flow agreed well with known values (~80%) for both groups, however, these are meaningless parameters in the setting of hepatofugal flow, which was the case of one of the patients (** in Figure 6). Finally, the error observed using the conservation of mass measurements was relatively small, demonstrating internal consistency of the flow measurements at the portal confluence, bifurcation and within the portal vein. These small errors may have been due to very small tributary vessels to the portal vein, or small early branches that were not identified.

Limitations of this study include the relatively small number of subjects and the lack of control for stage of cirrhosis or etiology of liver disease. In addition, post-processing of the velocity data sets currently requires relatively intense user-computer interaction, typically requiring 2 hours from an experience operator. Further, semi-automatic segmentation, as was used here, is subjective and may result in non-visualization of some small vessels. This may lead to small apparent errors in the conservation mass calculations.

An additional limitation of this study is that no repeatability experiments were performed to determine the precision of radial 4D flow MRI for quantifying flow in the portal and splanchnic circulation. Determination of the precision will be essential before widespread clinical use of these methods can be implemented, in order to understand the magnitude of change that can be measured reliably. Unfortunately, the additional scan time required to perform the additional scanning needed to determine precision was not available within our experimental set-up. Future studies are currently being planned to measure this important characteristic of this quantitative biomarker.

Finally, a reference standard was not available for quantification of blood flow in the portal circulation that would allow us to validate our measurements. However, internal validation and consistency measurements using the conservation of mass principle provided excellent indirect validation. Validation with a gold standard reference would require invasive placement of flow probes.

Interestingly, conservation of mass at the portal confluence and bifurcation yielded a slope very close to, but slightly less than 1.0. This could be due to the presence of very small early branches distal to the SMV and SV measurement planes, and proximal to the RPV an LPV measurement planes. In both situations and in the presence of hepatopedal flow, the resulting error would lead to underestimation of $Q_{SMV} + Q_{SC}$ and $Q_{RPV}+Q_{LPV}$, respectively, and an apparent slope less than 1.0.

In conclusion, quantification of blood flow in the hepatic and splanchnic vasculature of patients with portal hypertension using radial 4D flow MRI with 5-point velocity encoding is very feasible. This approach provides a comprehensive, volumetric approach with high spatial resolution in reasonable scan time. Future work will focus on additional validation studies including larger comparison of patients with portal hypertension and controls, exploring clinical applications of these methods, and repeatability experiments.

Acknowledgments

The authors gratefully acknowledge support from the NIH (R01 DK083380, R01 DK088925 and RC1 EB010384), the University of Wisconsin Radiology R&D Committee, and GE Healthcare.

References

1. Centers for Desease Control and Prevention. 2009
2. Bhathal PS, Grossman HJ. Reduction of the increased portal vascular resistance of the isolated perfused cirrhotic rat liver by vasodilators. J Hepatol. 1985; 1(4):325–337. [PubMed: 4056346]
3. Zardi EM, Dobrina A, Uwechie V, et al. Postmeal portal flow variations in HCV-related chronic hepatitis and liver cirrhosis with and without hyperdynamic syndrome. In Vivo. 2008; 22(4):509–512. [PubMed: 18712180]
4. Moller S, Hobolth L, Winkler C, Bendtsen F, Christensen E. Determinants of the hyperdynamic circulation and central hypovolaemia in cirrhosis. Gut. 2011; 60(9):1254–1259. [PubMed: 21504996]
5. Burkart DJ, Johnson CD, Ehman RL, Weaver AL, Ilstrup DM. Evaluation of portal venous hypertension with cine phase-contrast MR flow measurements: high association of hyperdynamic portal flow with variceal hemorrhage. Radiology. 1993; 188(3):643–648. [PubMed: 8351326]
6. Thalheimer U, Bellis L, Puoti C, Burroughs AK. Should we routinely measure portal pressure in patients with cirrhosis, using hepatic venous pressure gradient (HVPG) as a guide for prophylaxis and therapy of bleeding and rebleeding? No. Eur J Intern Med. 2011; 22(1):5–7. [PubMed: 21238884]
7. Boyer TD. Changing clinical practice with measurements of portal pressure. Hepatology. 2004; 39(2):283–285. [PubMed: 14767977]
8. Stanley AJ, Robinson I, Forrest EH, Jones AL, Hayes PC. Haemodynamic parameters predicting variceal haemorrhage and survival in alcoholic cirrhosis. Qjm-Monthly Journal of the Association of Physicians. 1998; 91(1):19–25. [PubMed: 9519209]
9. Kim MY, Baik SK, Park DH, et al. Damping index of Doppler hepatic vein waveform to assess the severity of portal hypertension and response to propranolol in liver cirrhosis: a prospective nonrandomized study. Liver International. 2007; 27(8):1103–1110. [PubMed: 17845539]
10. Lebrec D, Hillon P, Munoz C, Goldfarb G, Nouel O, Benhamou JP. The effect of propranolol on portal hypertension in patients with cirrhosis: a hemodynamic study. Hepatology. 1982; 2(5):523–527. [PubMed: 6981575]
11. Patch D, Sabin CA, Goulis J, et al. A randomized, controlled trial of medical therapy versus endoscopic ligation for the prevention of variceal rebleeding in patients with cirrhosis. Gastroenterology. 2002; 123(4):1013–1019. [PubMed: 12360462]
12. Villanueva C, Aracil C, Colomo A, et al. Clinical trial: a randomized controlled study on prevention of variceal rebleeding comparing nadolol + ligation vs hepatic venous pressure gradient-guided pharmacological therapy. Aliment Pharmacol Ther. 2009; 29(4):397–408. [PubMed: 19006538]
13. Sanyal AJ. Hepatic venous pressure gradient: to measure or not to measure, that is the question. Hepatology. 2000; 32(5):1175–1176. [PubMed: 11050073]
14. Pomier-Layrargues, G.; Huet, P. Measurement of Hepatic Venous Pressure Gradient: Methods, Interpretation, and Pitfalls. In: Sanyal, A.; Shah, V., editors. Portal Hypertension: Pathobiology, Evaluation, and Treatment. Totowa, NJ: Humana Press; 2005. p. 141
15. Groszmann RJ, Wongcharatrawee S. The hepatic venous pressure gradient: anything worth doing should be done right. Hepatology. 2004; 39(2):280–282. [PubMed: 14767976]
16. D'Amico G, Garcia-Pagan JC, Luca A, Bosch J. Hepatic vein pressure gradient reduction and prevention of variceal bleeding in cirrhosis: A systematic review. Gastroenterology. 2006; 131(5): 1611–1624. [PubMed: 17101332]
17. Kamath PS, Tyce GM, Miller VM, Edwards BS, Rorie DK. Endothelin-1 modulates intrahepatic resistance in a rat model of noncirrhotic portal hypertension. Hepatology. 1999; 30(2):401–407. [PubMed: 10421647]

18. Feu F, Bordas JM, Luca A, et al. Reduction of variceal pressure by propranolol: comparison of the effects on portal pressure and azygos blood flow in patients with cirrhosis. Hepatology. 1993; 18(5):1082–1089. [PubMed: 8225212]
19. Conn HO, Grace ND, Bosch J, et al. Propranolol in the prevention of the first hemorrhage from esophagogastric varices: A multicenter, randomized clinical trial. The Boston-New Haven-Barcelona Portal Hypertension Study Group. Hepatology. 1991; 13(5):902–912. [PubMed: 2029994]
20. Bosch J, Masti R, Kravetz D, et al. Effects of propranolol on azygos venous blood flow and hepatic and systemic hemodynamics in cirrhosis. Hepatology. 1984; 4(6):1200–1205. [PubMed: 6500511]
21. Abraldes JG, Tarantino I, Turnes J, Garcia-Pagan JC, Rodes J, Bosch J. Hemodynamic response to pharmacological treatment of portal hypertension and long-term prognosis of cirrhosis. Hepatology. 2003; 37(4):902–908. [PubMed: 12668985]
22. Thuluvath PJ, Bal JS, Mitchell S, Lund G, Venbrux A. TIPS for management of refractory ascites: response and survival are both unpredictable. Dig Dis Sci. 2003; 48(3):542–550. [PubMed: 12757168]
23. Ganger DR, Klapman JB, McDonald V, et al. Transjugular intrahepatic portosystemic shunt (TIPS) for Budd-Chiari syndrome or portal vein thrombosis - Review of indications and problems. American Journal of Gastroenterology. 1999; 94(3):603–608. [PubMed: 10086638]
24. de Vries PJ, van Hattum J, Hoekstra JB, de Hooge P. Duplex Doppler measurements of portal venous flow in normal subjects. Inter- and intra-observer variability. J Hepatol. 1991; 13(3):358–363. [PubMed: 1808227]
25. Thabut D, Moreau R, Lebrec D. Noninvasive Assessment of Portal Hypertension in Patients With Cirrhosis. Hepatology. 2011; 53(2):683–694. [PubMed: 21274889]
26. Vizzutti F, Arena U, Rega L, et al. Performance of Doppler ultrasound in the prediction of severe portal hypertension in hepatitis C virus-related chronic liver disease. Liver International. 2007; 27(10):1379–1388. [PubMed: 18036101]
27. Paulson EK, Kliewer MA, Frederick MG, Keogan MT, DeLong DM, Nelson RC. Doppler US measurement of portal venous flow: variability in healthy fasting volunteers. Radiology. 1997; 202(3):721–724. [PubMed: 9051024]
28. Gouya H, Mallet V, Scatton O, et al. Magnetic Resonance Imaging (MRI) Flow, A New Non-Invasive Method for the Evaluation of Systemic, Splanchnic, and Azygos Blood Flows in Patients with Portal Hypertension. Hepatology. 2008; 48(4):1049A–1049A.
29. Wu MT, Pan HB, Chen C, et al. Azygos blood flow in cirrhosis: measurement with MR imaging and correlation with variceal hemorrhage. Radiology. 1996; 198(2):457–462. [PubMed: 8596849]
30. Stankovic Z, Frydrychowicz A, Csatari Z, et al. MR-based visualization and quantification of three-dimensional flow characteristics in the portal venous system. Journal of magnetic resonance imaging : JMRI. 2010; 32(2):466–475. [PubMed: 20677279]
31. Frydrychowicz A, Landgraf BR, Niespodzany E, et al. Four-dimensional velocity mapping of the hepatic and splanchnic vasculature with radial sampling at 3 tesla: A feasibility study in portal hypertension. Journal of magnetic resonance imaging : JMRI. 201110.1002/jmri.22712
32. Gu T, Korosec FR, Block WF, et al. PC VIPR: a high-speed 3D phase-contrast method for flow quantification and high-resolution angiography. AJNR Am J Neuroradiol. 2005; 26(4):743–749. [PubMed: 15814915]
33. Johnson KM, Markl M. Improved SNR in phase contrast velocimetry with five-point balanced flow encoding. Magn Reson Med. 2010; 63(2):349–355. [PubMed: 20099326]
34. Johnson KM, Francois C, Lum D, et al. Rapid comprehensive evaluation of luminography and hemodynamic function with 3D radially undersampled phase contrast imaging MRI. Conf Proc IEEE Eng Med Biol Soc. 2009; 1:4057–4060. [PubMed: 19964098]
35. Liu J, Redmond MJ, Brodsky EK, et al. Generation and visualization of four-dimensional MR angiography data using an undersampled 3-D projection trajectory. IEEE Trans Med Imaging. 2006; 25(2):148–157. [PubMed: 16468449]
36. Bernstein MA, Xiaohong JZ, Zhou J, et al. Concomitant gradient terms in phase contrast MR: Analysis and correction. Magn Reson Med. 1998; 39(2):300–308. [PubMed: 9469714]

37. Walker PG, Cranney GB, Scheidegger MB, Waseleski G, Pohost GM, Yoganathan AP. Semiautomated method for noise reduction and background phase error correction in MR phase velocity data. Journal of magnetic resonance imaging : JMRI. 1993; 3(3):521–530. [PubMed: 8324312]

38. Johnson KM, Lum DP, Turski PA, Block WF, Mistretta CA, Wieben O. Improved 3D phase contrast MRI with off-resonance corrected dual echo VIPR. Magn Reson Med. 2008; 60(6):1329–1336. [PubMed: 19025882]

39. Stalder AF, Russe MF, Frydrychowicz A, Bock J, Hennig J, Markl M. Quantitative 2D and 3D phase contrast MRI: optimized analysis of blood flow and vessel wall parameters. Magn Reson Med. 2008; 60(5):1218–1231. [PubMed: 18956416]

40. Chow PK, Yu WK, Soo KC, Chan ST. The measurement of liver blood flow: a review of experimental and clinical methods. J Surg Res. 2003; 112(1):1–11. [PubMed: 12873426]

41. Ludwig D, Schwarting K, Korbel CM, Bruning A, Schiefer B, Stange EF. The postprandial portal flow is related to the severity of portal hypertension and liver cirrhosis. J Hepatol. 1998; 28(4): 631–638. [PubMed: 9566832]

42. Siringo S, Piscaglia F, Zironi G, et al. Influence of esophageal varices and spontaneous portal-systemic shunts on postprandial splanchnic hemodynamics. The American journal of gastroenterology. 2001; 96(2):550–556. [PubMed: 11232705]

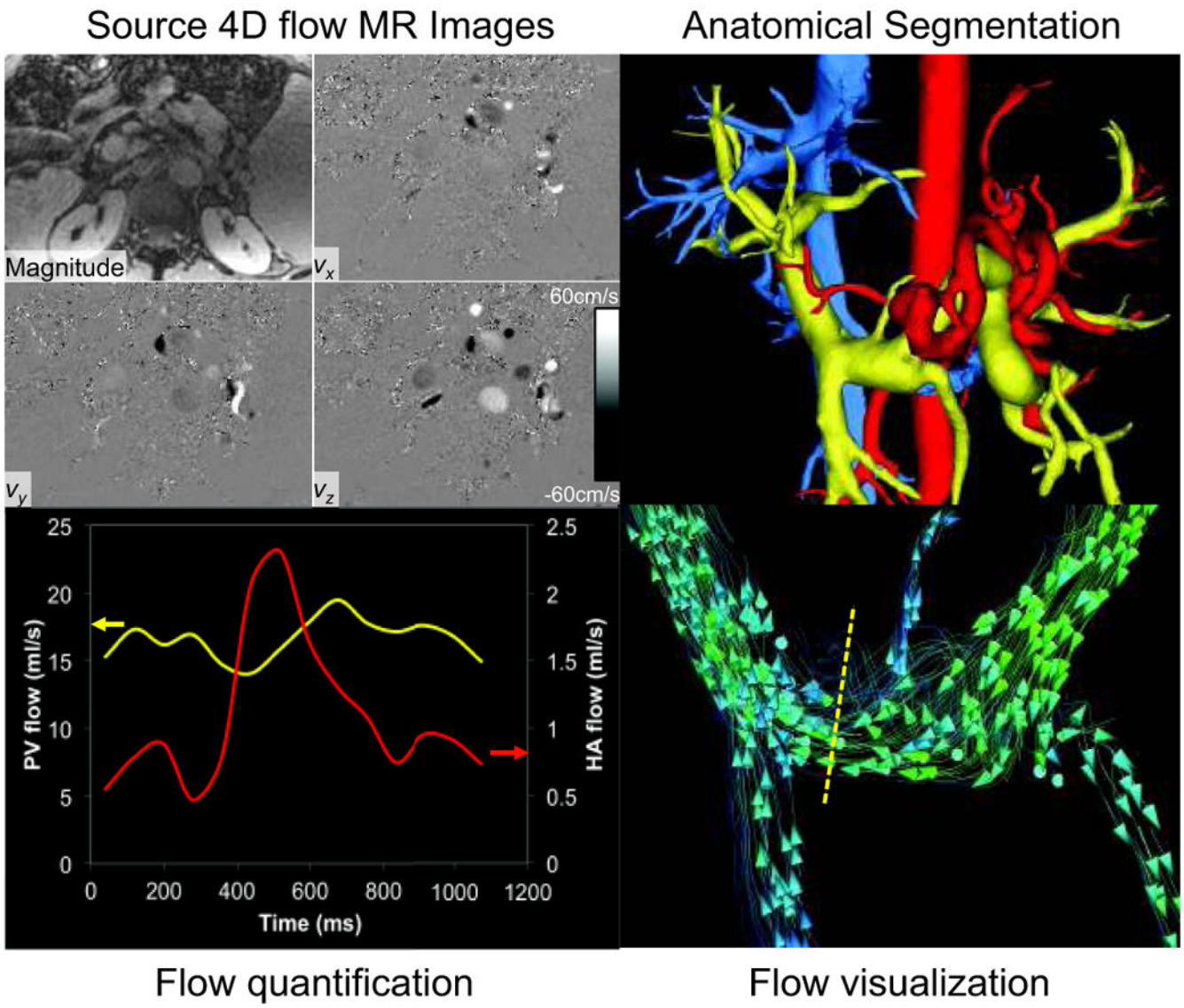

Figure 1.

Visualization of abdominal hemodynamics using 4D flow MRI. Workflow starts with source magnitude and velocity images (upper left, axial plane), which are combined into an anatomical PC angiogram (PCA) using complex difference processing. The PCA is segmented into color-coded vascular territories (Upper right), followed by streamline or particle trace visualization (bottom right). Note the cut-lanes perpendicular to the direction of the flow in the vessels of interest. Flow in the vessel of interest, in this case blood flow in the hepatic artery, is measured from flow waveforms using a Matlab-based tool (bottom left).

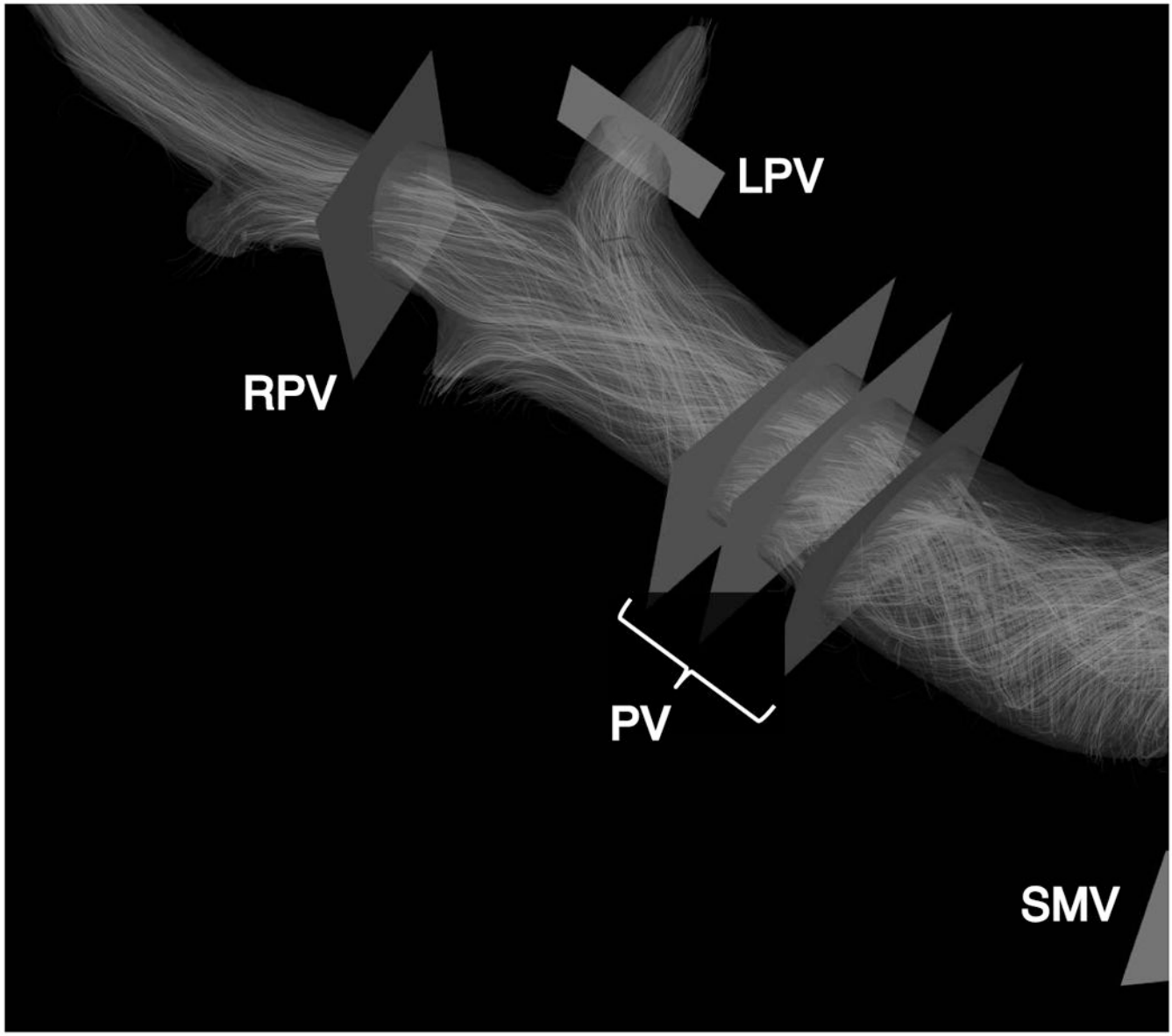

Figure 2.

Conservation of mass at the portal confluence and within the main portal vein for indirect validation of flow measurement accuracy. Flow in the portal vein (Q_{PV}) should be approximately equal to the flow in the splenic (Q_{SV}) and superior mesenteric vein (Q_{SMV}) added.

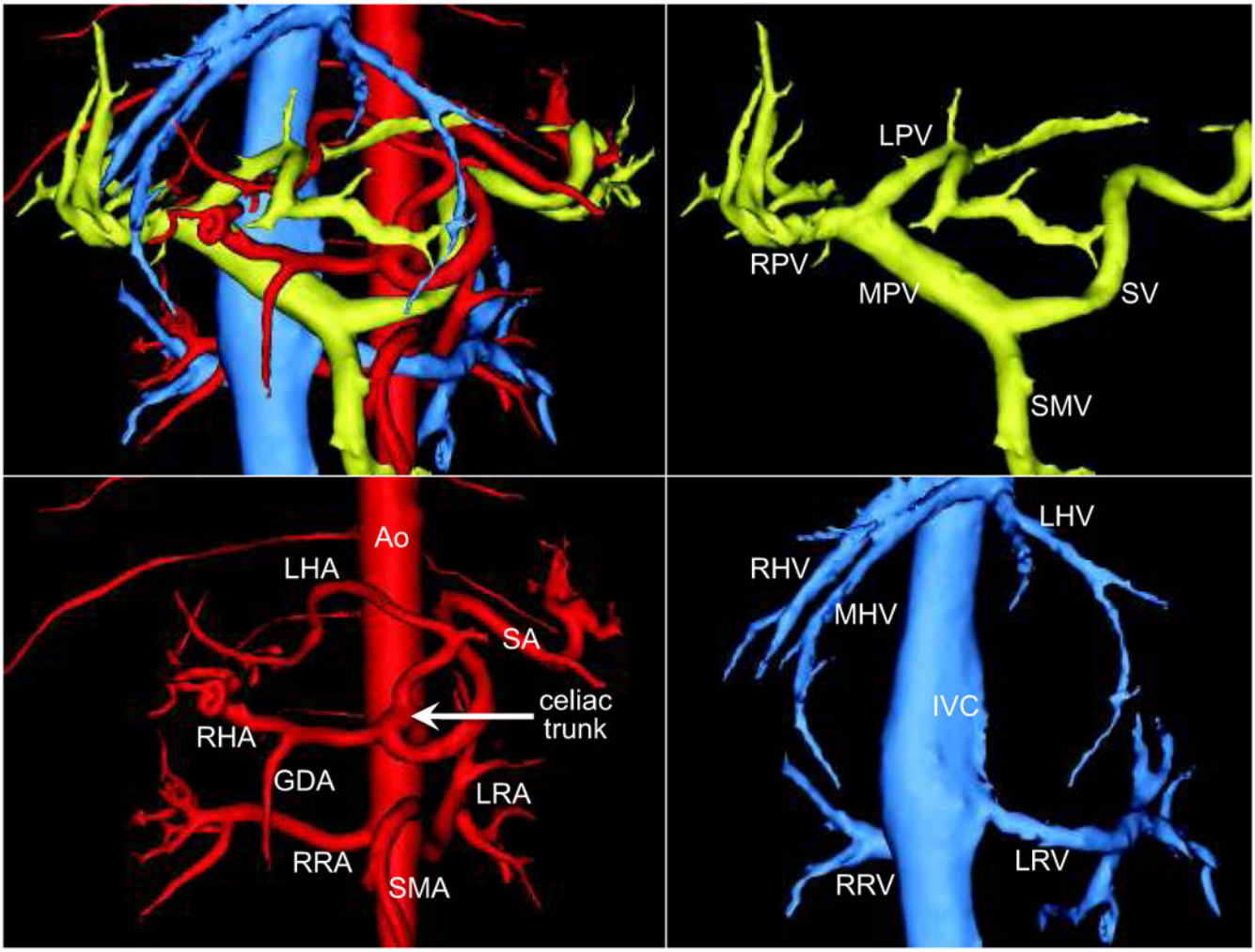

Figure 3.

The hepatic vasculature is complex and variable. Segmented 4D flow MR images provide 3D visualization of vascular anatomy. Note the replaced LHA, a normal variant, and visualization of the RRA and LRA. (MPV=main portal vein, RPV=rt. PV, LPV=lt. PV, SV=splenic vein, SMV = superior mesenteric vein, Ao=aorta, RRA=rt. renal artery, LRA=lt. RA, RHA=rt. hepatic artery, LHA=lt. hepatic artery, SA=splenic artery, SMA=superior mesenteric artery, IVC= inferior vena cava, RRV=rt. renal vein, LRV=lt. renal vein, RHV=rt. hepatic vein. MHV=middle HV, LHV=lt. HV).

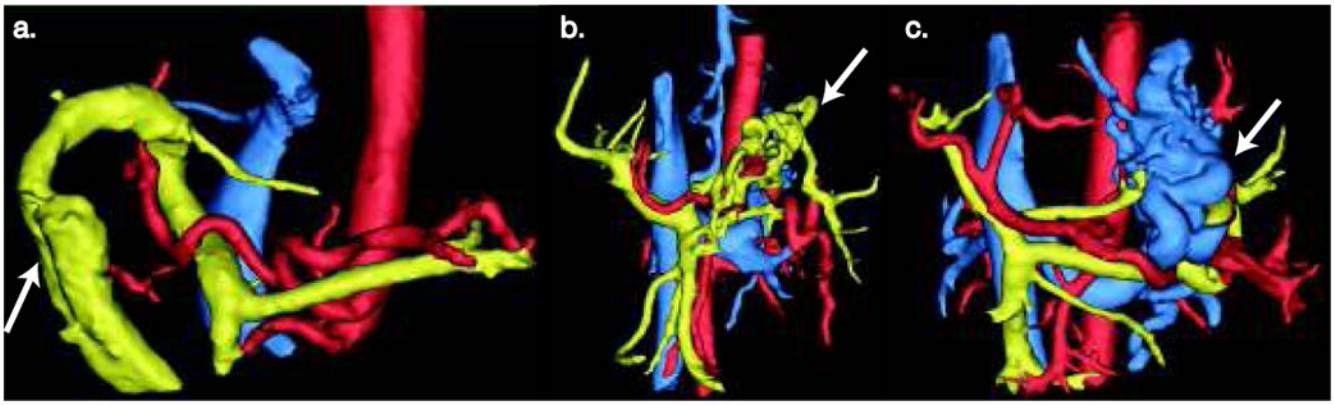

Figure 4.

Anatomical variations of the abdominal vasculature in patients with portal hypertension. a) Enlarged parahumbilical vein draining the portal vein (white arrow) b) Complex anatomy of the splenic vein (white arrow). c) Spleno-renal shunt (white arrow). Arterial circulation (Red), portal venous circulation (Yellow) and systemic venous circulation (Blue).

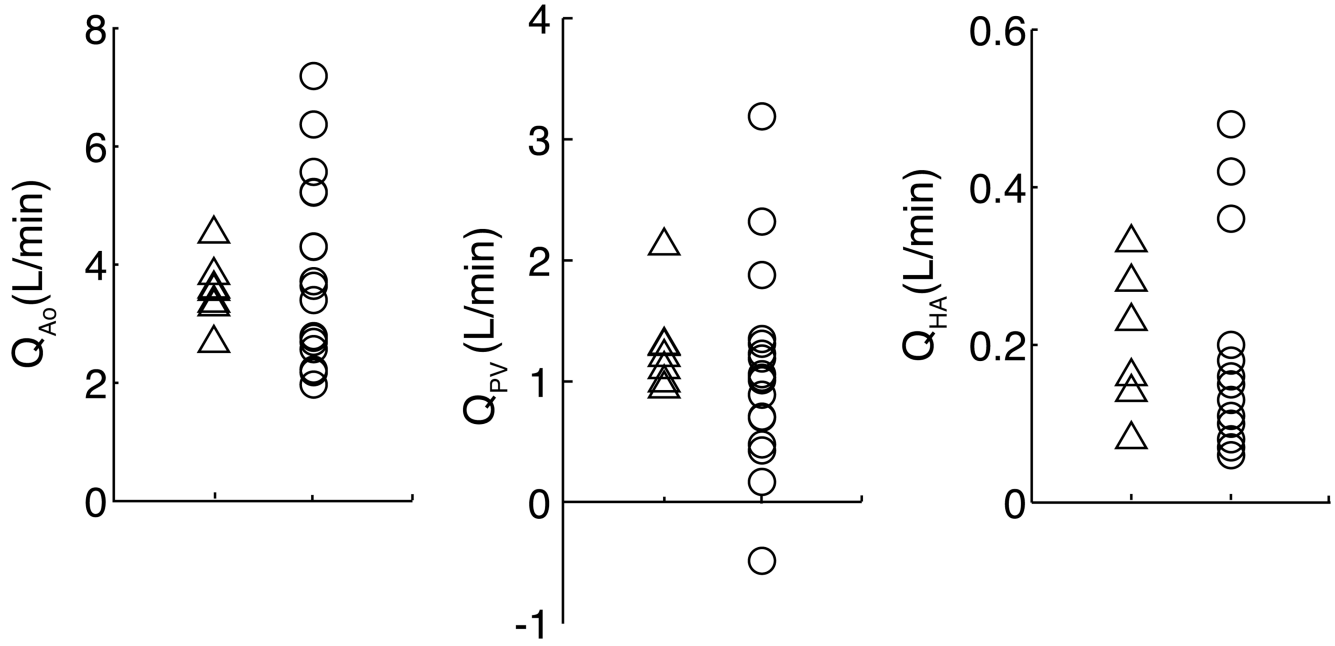

Figure 5.

Summary of the flow results in the abdominal aorta (Q_{Ao}) portal vein (Q_{PV}), hepatic artery (Q_{HA}). High variability of blood flow in the PV in patients with portal hypertension correlate well with the variability in blood flow in the abdominal aorta. Thus, variability in portal venous and hepatic arterial flow may be explained by differences in cardiac output due to variable presentation of a hyperdynamic state in patients with portal hypertension.

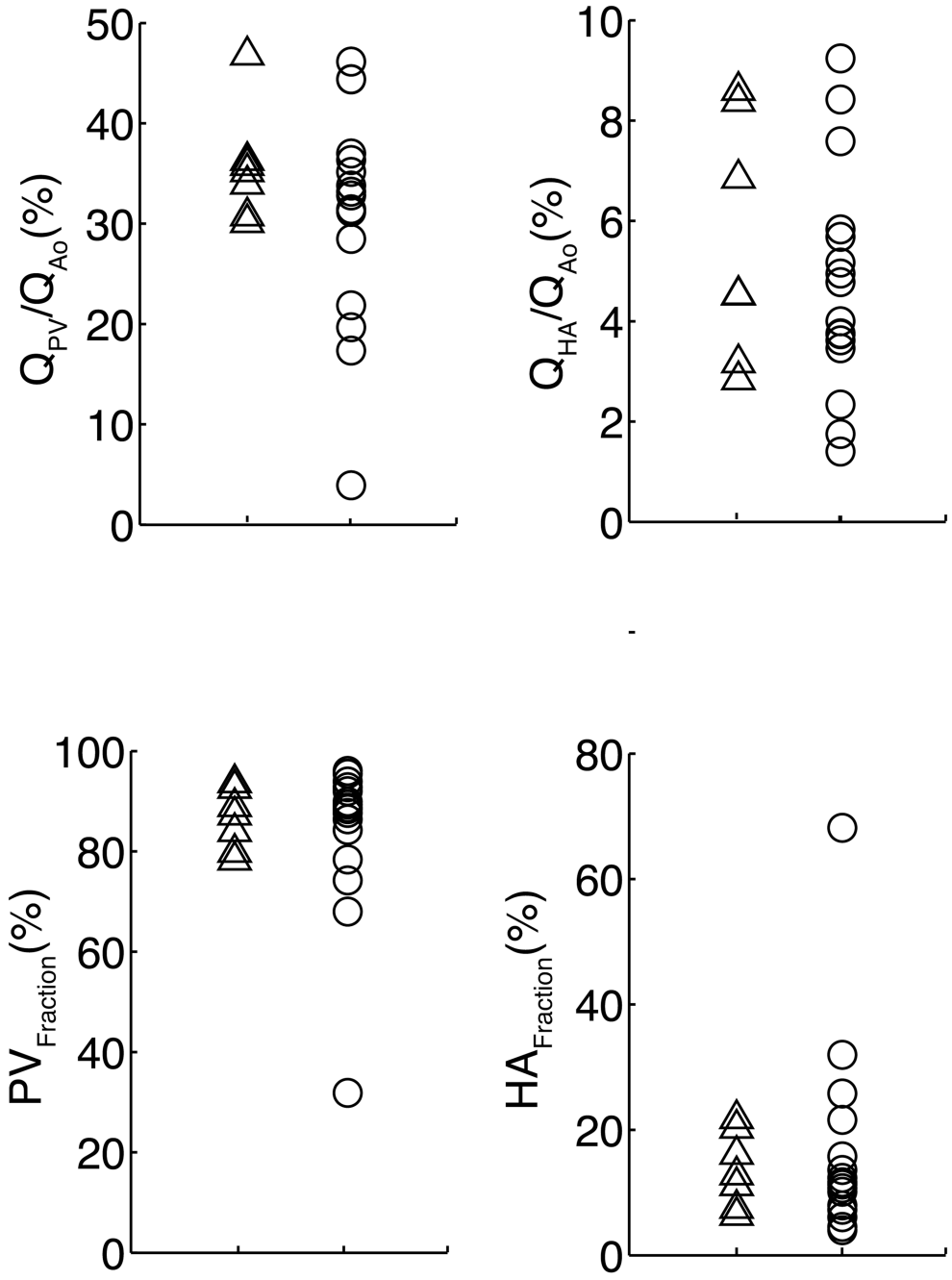

Figure 6.

Portal vein and hepatic artery flow normalized to abdominal aortic flow (Q_{PV}/Q_{Ao}) and Q_{PV}/Q_{Ao}). Individual contributions to total liver inflow ($Q_{PV}/(Q_{PV} + Q_{HA})$ and $Q_{HA}/(Q_{PV} + Q_{HA})$) show good agreement with data reported in the literature. Healthy controls are represented by triangles and circles represent patients with portal hypertension. (*) PH patient with reversed (hepato-fugal) Q_{PV} (HA fraction and PV fraction were not included for this patient since they are meaningless parameters in the setting of hepatofugal flow). (**) PH patient with markedely reduced Q_{PV} and reversed Q_{SV}.

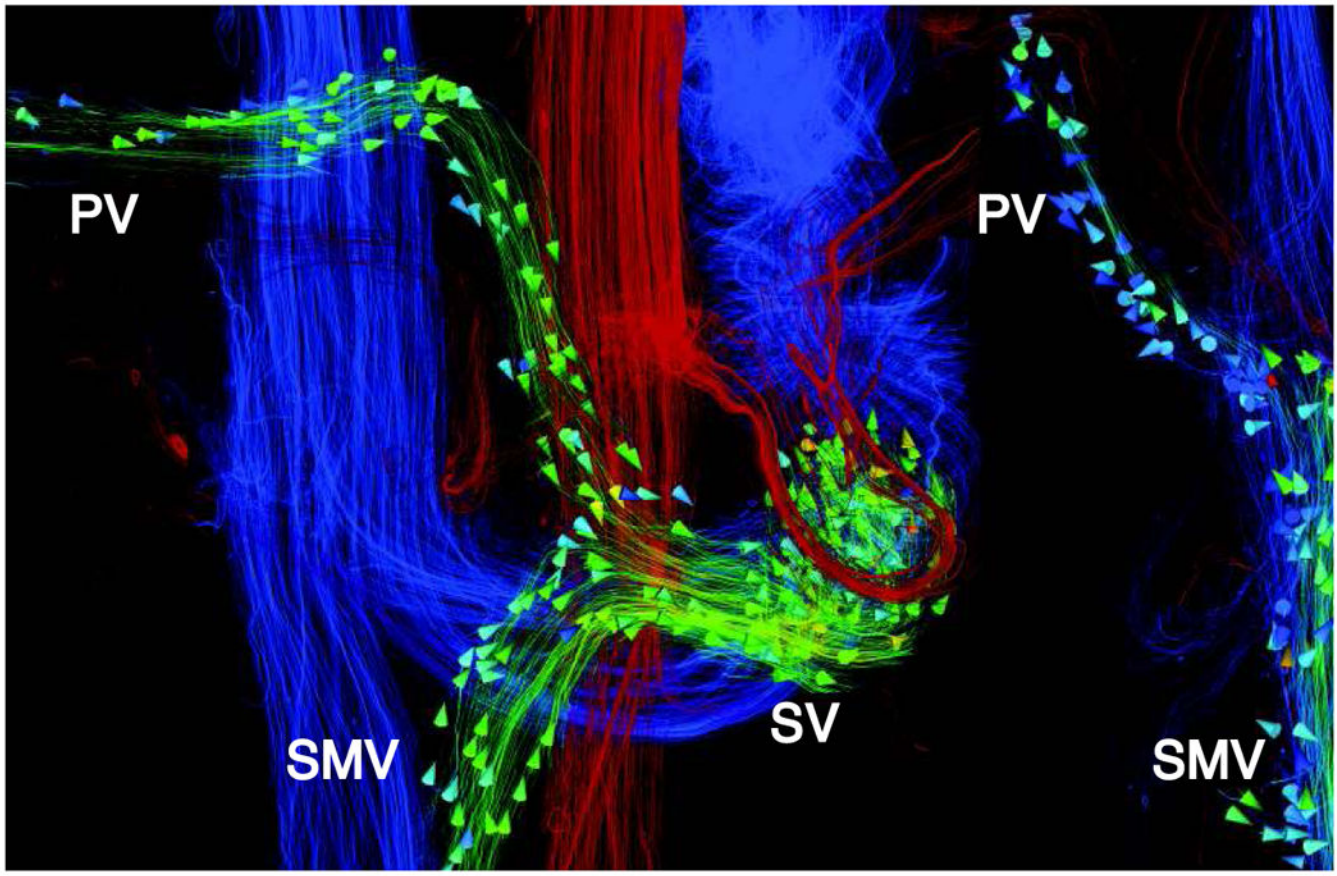

Figure 7.

Physiological variation in blood flow through the portal vein due to the increase resitance in two patients with portal hypertension. a) Reversed (hepato-fugal) flow is seen in the portal and splenic veins (** in Fig.6). Conservation of mass analysis showed good agreement (4.57%) between Q_{PV} and $Q_{SMV} + Q_{SV}$. b) Reversed Q_{SV} with reduced Q_{PV} and normal Q_{SMV} (* in Fig.6). Reversed flow can also be seen in the coronary vein in this patient.

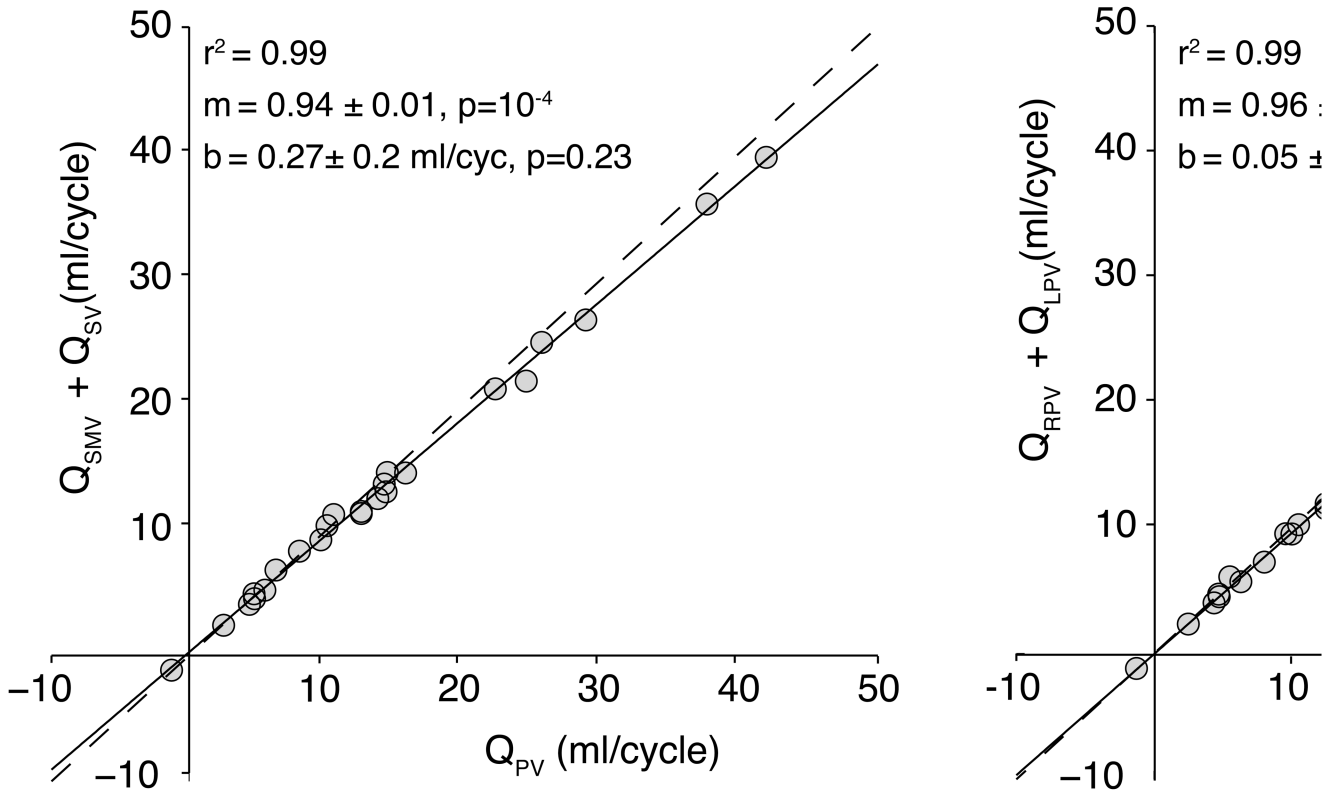

Figure 8.

Conservation mass validation. a. Portal confluence flow ($Q_{PV} \sim Q_{SMV} + Q_{SV}$). b. Portal bifurcation ($Q_{PV} \sim Q_{RPV} + Q_{LPV}$). Dashed line represents unity.